Relative Entropy Application to Study the Elastoplastic Behavior of the S235JR Structural Steel

Marcin Kamiński * and Michał Strąkowski

Posted Date: 29 November 2023

doi: 10.20944/preprints202311.1880.v1

Keywords: Stochastic Finite Element Method; Ramberg-Osgood material model; stochastic perturbation technique; Monte–Carlo simulation; semi-analytical method; Least Squares Method

Article

Relative Entropy Application to Study the Elastoplastic Behavior of the S235JR Structural Steel

Marcin Kamiński [1,*] and Michał Strąkowski [2]

[1] Department of Structural Mechanics, Faculty of Civil Engineering, Architecture and Environmental Engineering, Łódź University of Technology, Chair of Structural Reliability, 90-924 Łódź, Poland
[2] Department of Structural Mechanics, Faculty of Civil Engineering, Architecture and Environmental Engineering, Łódź University of Technology, 90-924 Łódź, Poland; michal.strakowski@p.lodz.pl
* Correspondence: marcin.kaminski@p.lodz.pl; Tel.: +48-42-631-3571

Abstract: The main issue in this work is to study limit functions necessary for the reliability assessment of the structural steel with the use of the relative entropy apparatus. This would be done using a few different mathematical theories relevant to this relative entropy, namely those proposed by Bhattacharyya, Kullback-Leibler, Jeffreys, and Hellinger. Probabilistic analysis in the presence of uncertainty in material characteristics would be delivered using three different numerical strategies – Monte-Carlo simulation, stochastic perturbation method as well as the semi-analytical approach. All these methods are based on the Weighted Least Squares Method approximations of the structural response functions versus the given uncertainty source and they would allow efficient determination of the first two probabilistic moments of the structural responses including stresses, displacements, and strains. The entire computational implementation would be delivered using the Finite Element Method system ABAQUS and computer algebra program MAPLE, where relative entropies, as well as polynomial response functions, would be determined. This study would demonstrate that the relative entropies may be efficiently used in reliability assessment close to the widely engaged First Order Reliability Method (FORM).

Keywords: stochastic finite element method; Ramberg-Osgood material model; stochastic perturbation technique; Monte–Carlo simulation; semi-analytical method; least squares method

1. Introduction

Structural materials and engineering structures exhibit a lot of various uncertainty sources ranging from environmental actions (as mechanical and/or thermal loadings), material statistical imperfections as well as some initial or manufacturing inaccuracies resulting in a necessity of the reliability assessment [1]. This can be done also both on structural or on the given material level, which is especially remarkable in composite materials area but occurs also in classical civil engineering materials like structural steels. A situation is complex in the case of metallic materials due to their apparent nonlinearity under the mechanical loads and exploitation temperatures variations on the one hand, and the need of the cross-sections optimization on the other. This leads to frequent application of nonlinear constitutive laws like Ramberg-Osgood having numerous applications [2–12], which can be also applicable in the soil engineering [13]. Alternatively, one may employ Johnson-Cook, especially convenient for higher temperatures (traditional and modified formulations) [14] or Gurson-Tvergaard-Needleman [15] (including porosity in metal microstructures) in the modern Finite Element Method (FEM) [16] simulations calibrated to the experimental data. Some more advanced modern theories include fractional plasticity models [17].

A majority of the Ramberg-Osgood model is in the fact that it has a single parameter needing experimental verification, so its usage seems to be very efficient, not only in the field of steel structures, but also in geotechnical applications. Such a nonlinear analysis becomes very complex where any uncertainty sources appear in the model – they can follow material micro, nano or

 doi:10.20944/preprints202311.1880.v1

molecular scales defects, but also more classical statistical discrepancies in structural elements lengths, location of the openings, holes, welds or some inclusions [18,19]. Mechanical properties' randomness in structural steel elements experimentation is most frequently noticed in Young modulus and yield strength, which directly follow unidirectional extension of the series of specimens. Standard deviations obtained for the brand new elements are obviously remarkable smaller than for the specimens cut from the extensively exploited structural elements under supervision, where additionally corrosion process may destruct both – geometry and material structure.

It is well known that several mathematical and numerical methods have been established in engineering mechanics to model the aforementioned phenomena and to predict their structural impacts. Close to the analytical calculus of the basic probabilistic parameters [20], Bayesian approach [21] and Monte-Carlo simulations family [22], one may find Karhunen-Loeve or polynomial chaos expansions [23], some semi-analytical techniques [20] as well as the group of stochastic perturbation methods [20,24]. The latter are formulated using various orders' approaches as the first, the second, the third or general order Taylor expansions leading to determination of the first two, three of four basic statistics of structural behaviour. A general minority of all these techniques mentioned above resulting in the response statistics is a necessity of discussion of many parameters at the same time, which can be difficult and misleading. The alternative way is to directly investigate a failure danger by its probability, which remains less useful in practical engineering reliability assessment; some solution to this problem may be determination of probabilistic entropy, whose fluctuations in mechanical problems enables uncertainty propagation discussion. More popular models include Shannon [25], Renyi [26] and Tsallis [27] models together with their further modifications and improvements.

Quite a similar situation takes place in reliability and durability studies, where the moment methods prevail [28]. the First Order Reliability Method (FORM) [29] convenient mostly for linear limit functions has been replaced with time by the second order methodology (SORM) [30], and even by the First [31] or the Second Order Third Moment (SOTM) technique [32]. The very interesting opportunity is the so-called probabilistic divergence (relative entropy) [33], which enables to quantify with some single real value a distance in-between two random distributions while having their probability distributions or the basic probabilistic characteristics. Unfortunately, a comparison between FORM and SORM and relative entropies apparatus is rather scarce in the literature, which follows mainly remarkable number of total different mathematical concepts in that area. Nevertheless, relative entropy application seems to be more adequate because the final formula is sensitive to probability distributions type of both structural resistance and effort inherent in the limit function unlike in the FORM or SORM.

This study aims in reliability assessment in the well-known tension test of the structural steel specimen, which is numerically simulated using the Ramberg-Osgood stress-strain relationship implemented in the FEM system ABAQUS. Probabilistic analysis has been carried out here using polynomial functions relating extreme deformations and von Mises reduced stresses with Young modulus of the given steel type recovered numerically from several FEM tests with varying value of this parameter. Then, three different probabilistic methods, namely stochastic perturbation technique, semi-analytical method as well as Monte-Carlo simulation scheme have been engaged to determine the first four probabilistic coefficients of the structural response. The first two of them have been finally used to calculate the reliability indices according to the FORM technique, and also alternatively – thanks to the application of the Bhattacharyya [34], Hellinger [35], Jeffreys [36,37] and Kullback-Leibler [38,39] relative entropies. As it has been documented classical FORM analysis may find its efficient alternatives in modern computer aided engineering of the steel details and structures. The results obtained here for Gaussian input uncertainty may be extended towards non-Gaussian distributions [40] also with minor modifications of numerical apparatus.

Preprints (www.preprints.org) | NOT PEER-REVIEWED | Posted: 29 November 2023 doi:10.20944/preprints202311.1880.v1

2. Theoretical Background

2.1. Governing Equations

The following incremental boundary value problem is considered in certain solid body domain Ω having continuous and sufficiently smooth boundary ∂Ω [41]:

$$\Delta\sigma_{kl,l} + \rho\Delta f_k = 0\,;\ \ \mathbf{x} \in \Omega \tag{1}$$

$$\Delta\sigma_{kl} = C_{klmn}\Delta\varepsilon_{mn}\,;\ \ \mathbf{x} \in \Omega \tag{2}$$

$$\Delta\varepsilon_{mn} = \tfrac{1}{2}\left\{\Delta u_{k,l} + \Delta u_{l,k} + u_{i,k}\Delta u_{i,l} + \Delta u_{i,k}u_{i,l} + \Delta u_{i,k}\Delta u_{i,l}\right\}\,;\ \ \mathbf{x} \in \Omega \tag{3}$$

for i, j, k, l =1,2,3 with the following boundary conditions:

$$\Delta\sigma_{\bar{k}l}n_l = \Delta t_{\bar{k}}\,;\ \ \mathbf{x} \in \partial\,\Omega_\sigma\,,\ \ \bar{k} = 1,2,3 \tag{4}$$

$$\Delta u_{\hat{k}} = \Delta\hat{u}_{\hat{k}}\,;\ \ \mathbf{x} \in \partial\,\Omega_u\,,\ \ \hat{k} = 1,2,3 \tag{5}$$

This problem is solved for the displacement vector $u_k(\mathbf{x})$, the strain tensor $\varepsilon_{kl}(\mathbf{x})$ and the stress tensor $\sigma_{kl}(\mathbf{x})$, a symbol Δ denotes their increments, while the fourth-rank tensor C_{klmn} denotes here a constitutive tensor. This solution is achieved using the appropriate incremental version of the potential energy functional, and their minimization with respect to the displacement vector. Classical FEM discretization for nonlinear problems has been proposed with many numerical illustrations in [42]. The entire probabilistic approach is based upon deterministic series of solutions of the iterative deterministic FEM equation as follows [43]

$$\mathbf{K}^{(m)}\Delta\mathbf{q}^{(m)} = \Delta\mathbf{Q}^{(m)} \tag{6}$$

where **K** denotes the stiffness matrix, Δ**Q** is the nodal loads' increments vector, whereas Δ**q** stands for the displacements vector increments; m indices here a current FEM test number necessary for the Response Function Method recovery of polynomial bases. These bases are approximated via the Least Squares Method [44] from the series of the FEM experiments with some input parameters varying throughout their fluctuations ranges, which have been assumed a priori.

A phenomenological constitutive model is analyzed here and it is known in the literature as the Ramberg-Osgood equation. It connects unidirectional strain ε with the tensile stress σ using the following well-known formula:

$$\varepsilon = \frac{\sigma}{E} + \alpha\frac{\sigma}{E}\left(\frac{\sigma}{f_y}\right)^{n-1} \tag{7}$$

where f_y denotes the yield strength of the given material, E is its Young modulus, α corresponds to the yield effect and n is the non-dimensional strain hardening coefficient. Quite naturally E and/or f_y may be perceived as some uncertainty sources because their mean values and other statistics result from the strength experiments with the well-documented statistics. However, derivation of any of the probabilistic analytical constitutive formulas would be rather difficult in this context as the uncertainty sources appear independently (or commonly) in the denominator of the aforementioned equation.

Visualization of the Ramberg-Osgood equation in its deterministic version is proposed below – in Figure 1. This figure includes two graphs – the left one contains the stress-strain curves for three different structural sheets of steel, namely S235, S355, and S460 plotted for the material coefficients α=0.002, which is normative plastic strain according to Eurocode 3-1-1 and also with n=0.20 (adopted experimentally). The right graph is adjacent to the elastoplastic behavior of the weakest steel, S235, while modifying the strain hardening coefficient by only. It is seen that the importance of this second

Preprints (www.preprints.org) | NOT PEER-REVIEWED | Posted: 29 November 2023 doi:10.20944/preprints202311.1880.v1

parameter is more remarkable, especially at the early stages of deformation. An influence of the yield strength is generally smaller but is kept on almost the same level until the specimen failure.

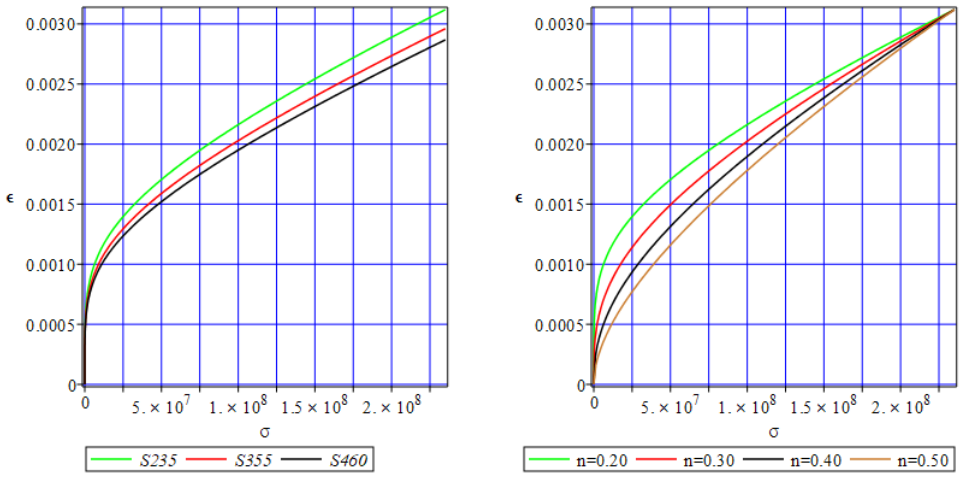

Figure 1. Stress-strain curves according to Ramberg-Osgood law for different structural steels (left) and sensitivity of S235 to the strain hardening coefficient (right).

Generally, the elastoplastic analysis may lead to structural failure, therefore reliability assessment gains a paramount importance. It engages the limit function relating structural resistance R and extreme structural response E in the range of given boundary conditions. Further numerical analysis takes into account the Serviceability Limit State (SLS) function based upon the extreme and admissible displacements in the given specimen, and also Ultimate Limit State (ULS) reduced von Mises stress and the corresponding yield strength of the structural steel under consideration. One may recall a definition of the reliability index due to the Cornell first-order theory as [31]

$$\beta(R,E)=\frac{E[R]-E[E]}{\sqrt{Var(R)+Var(E)-2Cov(R,E)}}, \tag{8}$$

which uses the first two probabilistic moments of both R and E, namely their expectations $E[.]$ and variances $Var(.)$. Determination of the expectations and variances of extreme displacements and of extreme reduced stresses undergoes through the series of the FEM experiments enabling for polynomial representation of these state functions with respect to the given uncertainty sources. Such a polynomial basis is sought using the Least Squares Method and enables further triple probabilistic calculus, where (*i*) its analytical integration with probability kernel is the basis for the semi-analytical method, (*ii*) its Taylor series expansion leads to the stochastic perturbation scheme, and also (*iii*) random number generation and sequential processing of this polynomial statistical estimators.

It is well-known that the FORM methodology has its limitations so its alternative is frequently sought. Probabilistic divergence (entropy) between two different probability distributions may apply for this purpose, and Bhattacharyya theory contains the following to quantify the distance from E to R [34]:

$$H_B(R,E)=\frac{1}{4}\frac{\left(E[R]-E[E]\right)^2}{\sigma^2(R)+\sigma^2(E)}+\frac{1}{2}\ln\left(\frac{\sigma^2(R)+\sigma^2(E)}{2\sigma(R)\sigma(E)}\right) \tag{9}$$

A comparison of these last two formulas exemplifies a need and suggests the way of upscaling of the entropy $H(R,E)$ to the FORM reliability index fluctuations level. There holds

$$\beta=2\sqrt{\frac{1}{4}\frac{\left(E[R]-E[E]\right)^2}{\sigma^2(R)+\sigma^2(E)}+\frac{1}{2}\ln\left(\frac{\sigma^2(R)+\sigma^2(E)}{2\sigma(R)\sigma(E)}\right)} \tag{10}$$

Preprints (www.preprints.org) | NOT PEER-REVIEWED | Posted: 29 November 2023 doi:10.20944/preprints202311.1880.v1

It is seen that the entropy-based approach reduces to the FORM one when both uncertainty levels in R and E are equal to each other. This particular entropic approach follows a general formula given for two probability distributions of the variables R and E:

$$H_B\left(p(R),p(E)\right)=\int_{-\infty}^{+\infty}\left\{p(R)(x)\,p(E)(x)\right\}^{\frac{1}{2}}dx \tag{11}$$

This model has been found useful in some previous reliability assessments for structural elasto-static and elasto-dynamic designing problems, but some referential models have been proposed by Kullback & Leibler [38], Jeffreys [37] and Hellinger [35] have been contrasted here.

$$H_{KL}\left(p(R),p(E)\right)=-\int_{-\infty}^{+\infty}p(R)(x)\log\left(p(E)(x)\right)dx+\int_{-\infty}^{+\infty}p(E)(x)\log\left(p(R)(x)\right)dx \tag{12}$$

$$H_J\left(p(R),p(E)\right)=H_{KL}\left(p(R)(x),p(E)(x)\right)+H_{KL}\left(p(R)(x),p(E)(x)\right) \tag{13}$$

$$H_{SH}\left(p(R),p(E)\right)=\frac{1}{2}\int_{-\infty}^{+\infty}\left(\sqrt{p(R)(x)}-\sqrt{p(E)(x)}\right)^2dx=1-\int_{-\infty}^{+\infty}\sqrt{p(R)(x)\,p(E)(x)}dx \tag{14}$$

Similarly to the Shannon entropy definitions, these entropies have been introduced for the non-truncated Gaussian distribution, which may result in some small modeling error in some engineering problems, where structural parameters exhibit truncated character. Moreover, it can be demonstrated that these entropies in case of two given different Gaussian probability distributions $p(R)\equiv N\left(E[R],\sigma(R)\right)$ $p(E)\equiv N\left(E[E],\sigma(E)\right)$ can be expressed in the following way (using their first two probabilistic moments only):

(*i*) Kullback-Leibler and Jeffrey's relative entropies

$$H_{KL}\left(p(R),p(E)\right)=\log\left(\frac{\sigma(E)}{\sigma(R)}\right)+\frac{\sigma^2(R)+\left(E[R]-E[E]\right)^2}{2\sigma^2(E)}-\frac{1}{2}, \tag{15}$$

$$\begin{aligned}H_J\left(p(R),p(E)\right)=&\log\left(\frac{\sigma(E)}{\sigma(R)}\right)+\frac{\sigma^2(R)+\left(E[R]-E[E]\right)^2}{2\sigma^2(E)}-1+\\&\log\left(\frac{\sigma(R)}{\sigma(E)}\right)+\frac{\sigma^2(E)+\left(E[E]-E[R]\right)^2}{2\sigma^2(R)}\equiv symm\left(H_{KL}\left(p(R),p(E)\right)\right)\end{aligned} \tag{16}$$

(*ii*) the squared Hellinger relative entropy

$$H_H\left(p(R),p(E)\right)=1-\sqrt{\frac{2\sigma(R)\sigma(E)}{\sigma^2(R)+\sigma^2(E)}}\exp\left(-\frac{1}{4}\frac{\left(E[R]-E[E]\right)^2}{\sigma^2(R)+\sigma^2(E)}\right). \tag{17}$$

Bhattacharyya entropy reduces in this case to Eqn (9) given above.

3. Numerical simulation of uniform extension of the steel cylinder

A standard tensile test was carried out. Figure 1 shows the geometry of the specimen. Because of the axisymmetric cross-section of the round bar, only one plain section of it was conducted. To ensure necking appears small notch made - it is a procedure well known from the literature [45]. 844 quadrilateral FEM elements known in the ABAQUS system as CAX4R (4-node bilinear axisymmetric element). Reduced integration has been used in this case. As can be seen, the bottom part of the specimen was discretized with smaller FEM elements. The side of the brick element is 0.5 mm. The top part of the sample is divided using finite elements with different sizes. Close to the rounding in the middle of the height the basic finite element size is 1.0 x 1.0 mm and is elongated to 1.0 x 2.0 mm on the top. It should be mentioned that some FEM studies are based on a combination of triangular (close to the necking) and quadrilateral elements (the remaining parts of the specimen) [15,16].

Preprints (www.preprints.org) | NOT PEER-REVIEWED | Posted: 29 November 2023 doi:10.20944/preprints202311.1880.v1

Figure 2 shows kinematic boundary conditions applied to the material specimen. The vertical displacements of the bottom edge are equal to zero (u_2=0), whereas horizontal displacements u_1=0 for the left edge being the symmetry axes. Kinematic boundary conditions of the top edge have been provided as the extending load and are introduced here as u_2=5.0 mm. The full Newton incremental method has been proposed to model incremental behavior in this case, and for this purpose an initial increment size was assumed 0.001, the minimum equal to 0.0001 and the maximum allowed increment size was 1. Obviously, large displacements have been allowed in this case study. All numerical experiments with ABAQUS have been carried out in Polish national network PL-Grid and approximate time consumption of the single incremental solution was about 5.0 minutes.

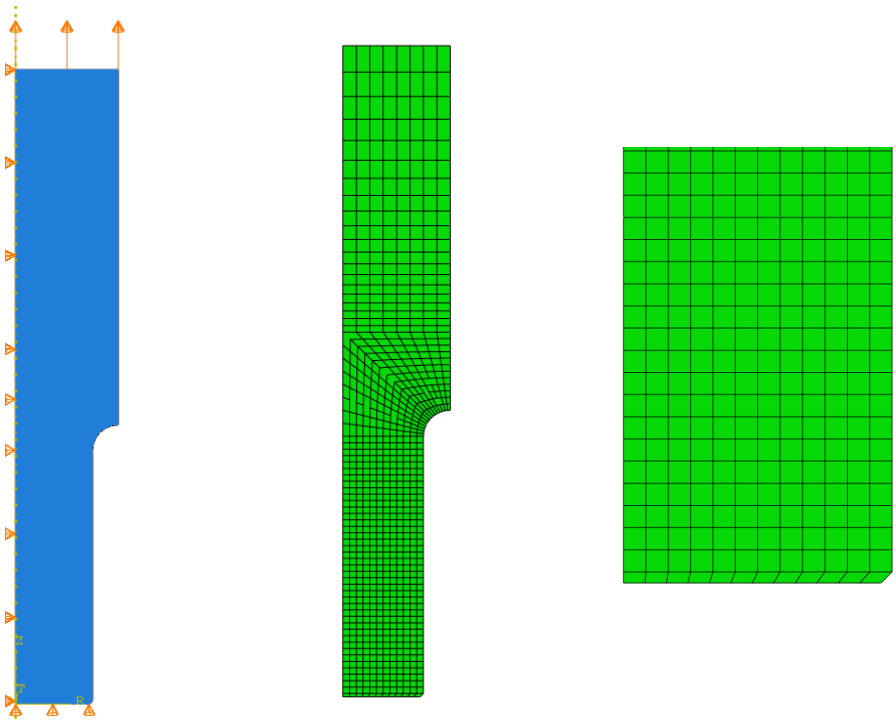

Figure 2. Geometry, boundary conditions, and meshing of the specimen.

Figure 3 presents the resulting von Mises stress distribution in a few selected stages of the analysis (beginning, in the middle and at its end). After 20% of the analysis (left drawing) bottom part of the specimen has stress close to ultimate strength f_u=360 MPa here. After 50-60 percent of the analysis (middle drawing) necking occurs, and the reduced stress reaches maximum values of 360 MPa. At the end of the analysis, necking is fully developed and maximum stress is concentrated in the vicinity of this cross-section.

Further part of numerical simulation has been delivered in the computer algebra system MAPLE, where the LSM approximation together with the three chosen probabilistic methods have been programmed. Additionally, the final part of the FORM and relative entropy computations have been also prepared in the same system by the script developed by the Authors. Most of the results have been presented below as the functions of increasing uncertainty introduced in the model, so that deterministic solutions are obtained as the lower bounds for all of these characteristics and largest scattering is the upper bound on the windows containing up to the fourth order characteristics and entropies.

Preprints (www.preprints.org) | NOT PEER-REVIEWED | Posted: 29 November 2023 doi:10.20944/preprints202311.1880.v1

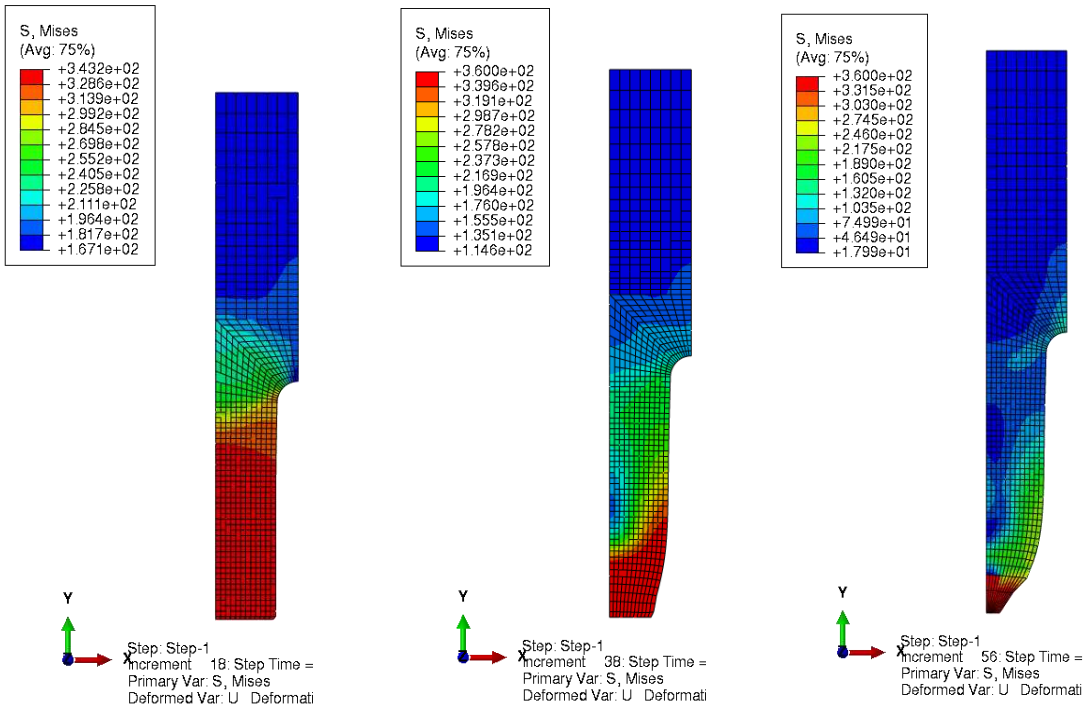

Figure 3. Resulting von Mises stress distribution for 20, 60, and 100% of the analysis progress.

Figure 4 presents response function polynomials of displacements (left one) dependent on Young modulus values from range 190,…,210,...,230 GPa. Such a relatively small dispersion causes displacements that are independent of the Young modulus. Moreover, displacements are concentrated around its mean values. The right part of Figure 4 shows response function method polynomials through the entire Young modulus dispersion, whereas shortly after about 30% of the analysis progress the resulting stress reaches maximum values 360 MPa. All the resulting polynomials are independent of the Young modulus. Further, this parameter is adopted as the main uncertainty source in our specimen, which follows a number of experimental works in civil engineering. Its mean value of 210 GPa has been further considered as the expected value, while the standard deviation has been adopted as 10% of this value, which agrees in many laboratory verifications. The second motivation for this choice is that this parameter is inherent in most of the civil engineering reliability studies as the design parameter, so it can be decisive for designing of most of more advanced structures, so that needs more attention.

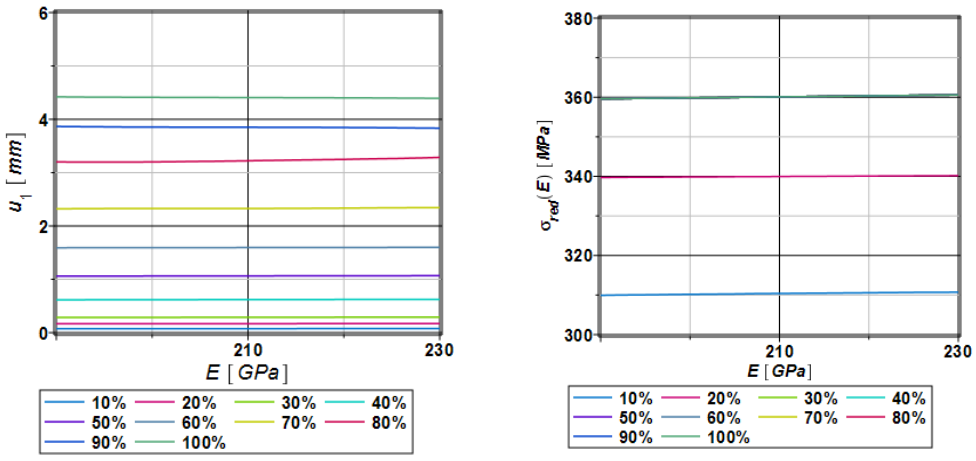

Figure 4. Response function polynomials of displacements and reduced stress as a function of the Young modulus E.

Preprints (www.preprints.org) | NOT PEER-REVIEWED | Posted: 29 November 2023 doi:10.20944/preprints202311.1880.v1

Figure 5 presents the distribution of the expectations of the extreme horizontal displacements as a function of the Young modulus E and those displacements follow the range of the necking. The perturbation method (PM), semi-analytical method (SAM), and Monte-Carlo Simulation (MCS) have been compared. At the beginning of the analysis, each method provides the same values of the necking concentrated round mean values. After about 70-80% of the process, some fluctuations can be observed. It can be identified with necking rapid expansion.

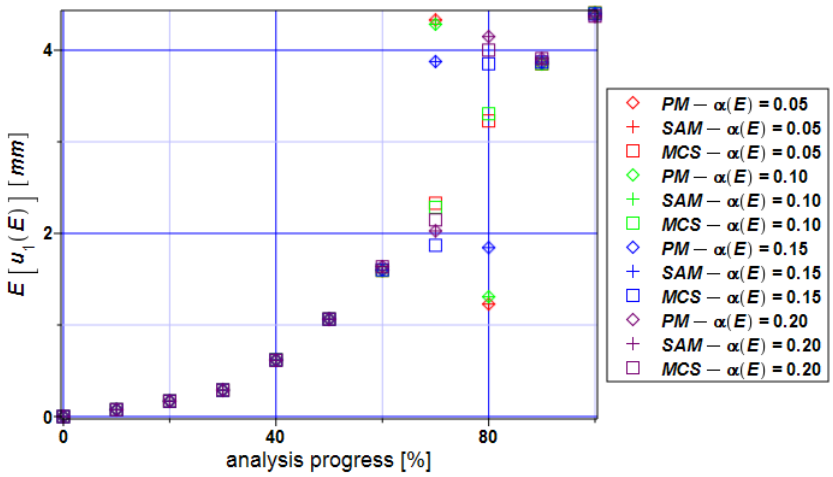

Figure 5. Expectations of the extreme displacements E[u1(E)] for the specimen.

Figure 6 shows the coefficients of the variation of the maximum horizontal displacements. Numerical values of this coefficient keep close to the input value throughout the entire analysis except the extreme input uncertainty, which results in enormously large displacements statistical scattering (close to even 4, which never happens in elasticity). These extreme coefficient of variation are noticed for about 70-80% - the absolute extreme has been noticed while using semi-analytical method, a little bit smaller value has been detected with the use of the Monte-Carlo simulation, whereas the perturbation method results in the minimum extreme value here.

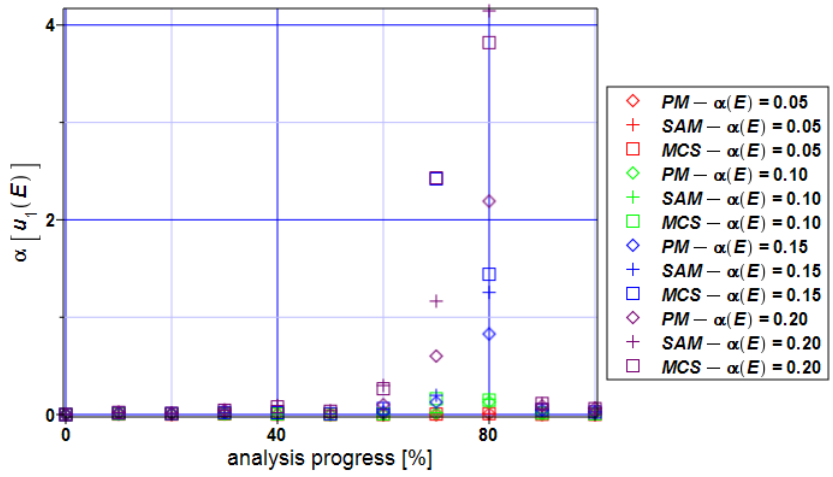

Figure 6. Coefficients of variation of the extreme displacements α[u1(E)] for the specimen.

Figure 7 presents the distribution of skewness values throughout the entire numerical experiment. At the beginning of this analysis, it takes values close to zero which tells us about the symmetry of the distribution of this state function. Skewness takes both positive and negative values for all three methods but most of them are positive. It tells us about the left-skewed distribution of the displacement state function. Skewness according to the perturbation method is close to zero if we narrow input CoV α(E)<0.15.

Preprints (www.preprints.org) | NOT PEER-REVIEWED | Posted: 29 November 2023 doi:10.20944/preprints202311.1880.v1

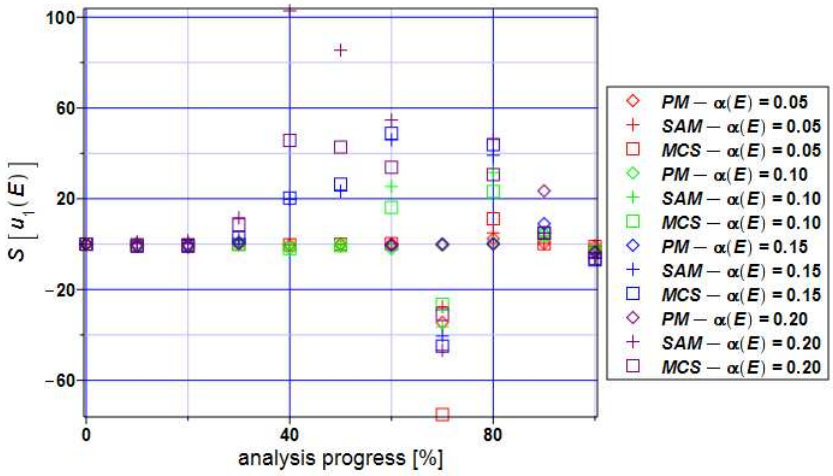

Figure 7. Skewness of the extreme displacements S[u1(E)] for the specimen.

Kurtosis of the horizontal displacements of the specimen (Figure 8) takes positive values according to all three methods. The perturbation method brings values of the kurtosis closest to zero. Semi-analytical method and Monte-Carlo Simulation take positive values of more than 2000 in the middle part of the analysis if $\alpha(E)>0.05$. The biggest positive values kurtosis takes for Monte-Carlo Simulation for $\alpha(E)=0.05$.

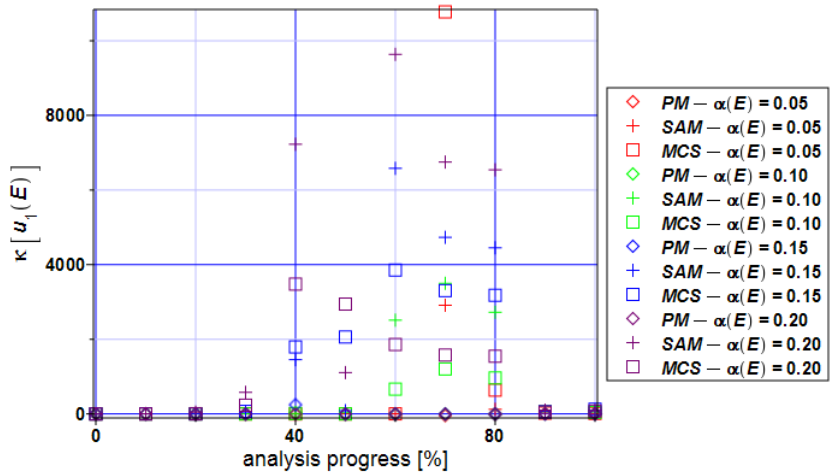

Figure 8. Kurtosis of the extreme displacements κ[u1(E)] for the specimen.

Figure 9 shows expectations of the von Mises reduced stress for the specimen. It can be seen that all three methods bring the same values which are very close to their means in a whole range of the input CoV $\alpha(E)=[0.05..0.20]$.

Preprints (www.preprints.org) | NOT PEER-REVIEWED | Posted: 29 November 2023 doi:10.20944/preprints202311.1880.v1

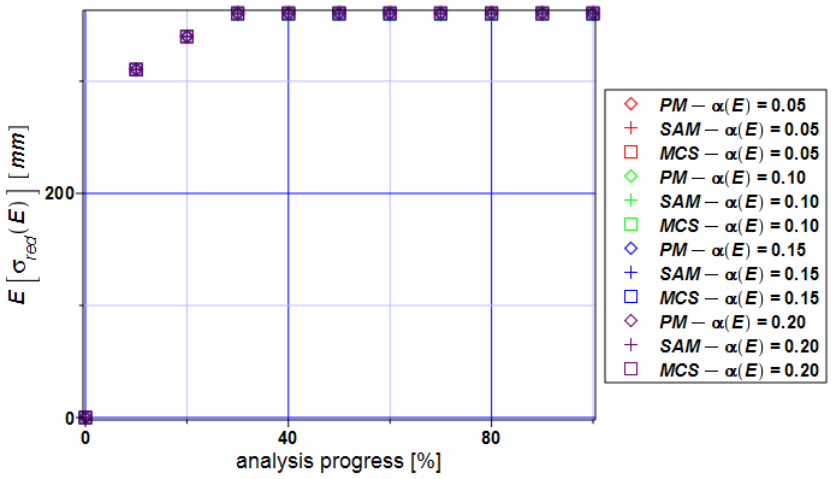

Figure 9. Expectations of the extreme reduced stress E[σ(E)] for the specimen.

The coefficient of variation of the reduced stress (Figure 10) is extremely close to zero based on all three methods. It means that expectations reflect mean values and this fact can be seen in Figure 9. Practically no uncertainty is observed in the reduced stresses here while contrasting these results with the series from Figure 6.

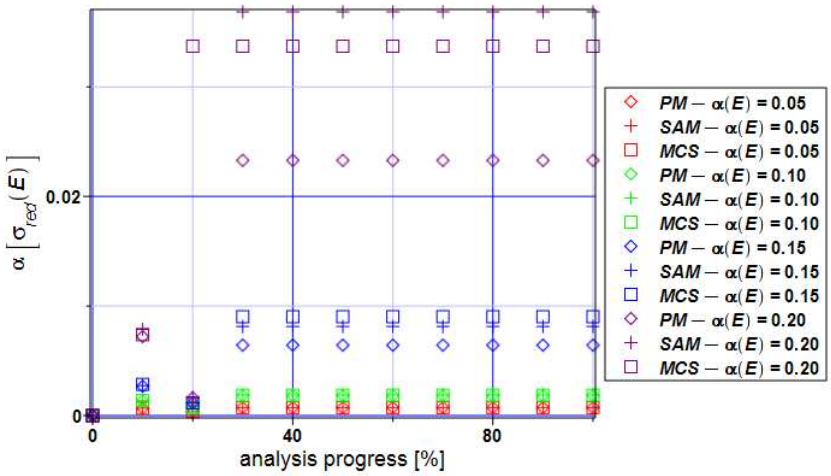

Figure 10. Coefficient of variation of the extreme reduced stress α[σ(E)] for the specimen.

Skewness contained in Figure 11 dominantly takes values close to zero if we limit the input coefficient of variation CoV to the values α(E)<0.10. Semi-analytical method and Monte-Carlo Simulation bring values larger than 20 for input CoV 0.15 and 0.20. Positive values of the skewness tell us that the distribution of von Mises reduced stress is left-skewed and should not be modelled using Gaussian PDF.

Preprints (www.preprints.org) | NOT PEER-REVIEWED | Posted: 29 November 2023 doi:10.20944/preprints202311.1880.v1

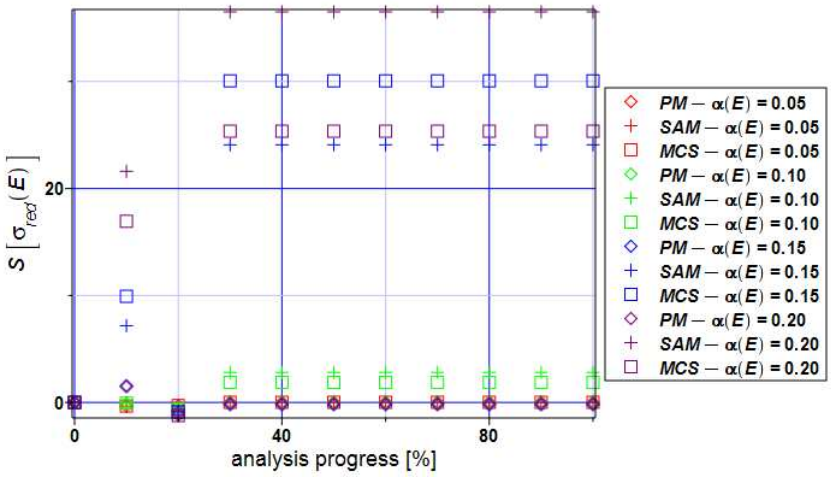

Figure 11. Skewness of the extreme reduced stress S[σ(E)] for the specimen.

Kurtosis of the extreme reduced stress (Figure 12) takes positive values throughout the entire extension process. Semi-analytical method and Mont-Carlo Simulation bring the values of the kurtosis in the range 2000-4000 for α(E)>0.10. It tells us that von Mises reduced stress distribution has long tails and peaks. If one bounds input CoV with α(E)≤0.05 then the distribution could be approximated by the Gaussian distribution with a relatively small modeling error.

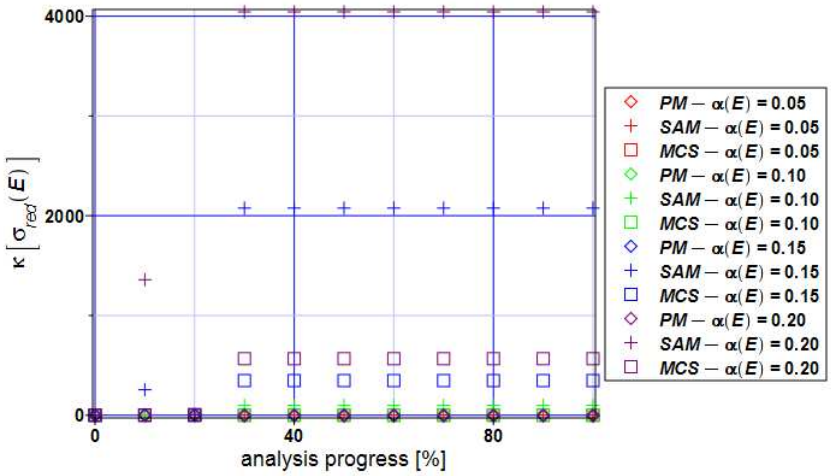

Figure 12. Kurtosis of the extreme reduced stress κ[σ(E)] for the specimen.

Figure 13 shows the reliability index distribution regarding displacements (left) and stress state (right). The red line is a safety level for normal, typical constructions. Reliability index β_u(E) takes the same values in a whole range of the input CoV. The amount of 90% of the specimen width has been taken as a limit value of the admissible extension (displacement). It is just an assumption because there is a complete lack of guidelines on how to calculate limit value. It can be observed that the specimen is in the failure region pretty fast (after 10 % of the analysis progress). But it relates to the expected values of the reduced stress (Figure 9). The values equal to the ultimate strength 360 MPa can be noticed at the beginning of the process (after 30-40%), while the stress equal to 360 MPa persists to the same end of numerical analysis. The specimen is close to the breaking and that's the reason why the reliability index takes values below the red line. One can see that the reliability index highly depends on the progress of nonlinear deformation, but it remains almost insensitive to the input CoV, α(E). Generally, bigger random dispersion in the specimen Young modulus leads to smaller values of the index β until its lowest admissible value is reached. Further, the reliability index decreases but

Preprints (www.preprints.org) | NOT PEER-REVIEWED | Posted: 29 November 2023 doi:10.20944/preprints202311.1880.v1

in an oscillating manner, and below the red limit we may observe some differences obtained for various statistical scattering in the input Young modulus.

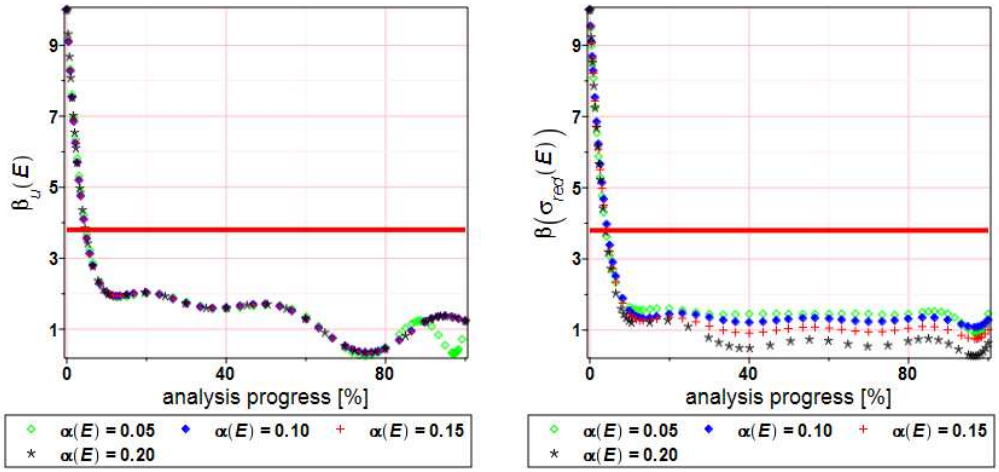

Figure 13. Reliability index of the displacements $\beta_u(E)$ and extreme reduced stress $\beta[\sigma(E)]$ for the specimen.

Figure 14 shows the relative entropy distribution for the horizontal displacements, where the input CoV has been taken from the interval α=[0..0.20], as before. The few relative entropies models developed by Bhattacharyya, Kullback-Leibler and Hellinger's have been compared with each other. During the entire analysis, the first two methods bring similar results. In the beginning, entropy reaches the values over 2500 for α<0.02. Then it decreases to minimum values at the end of the analysis. It has to be underlined that Hellinger equations provide smaller values of the relative entropy keeping close to 0 within the entire variability interval of the parameter α, and therefore, this relative entropy model seems to be less useful in reliability assessment.

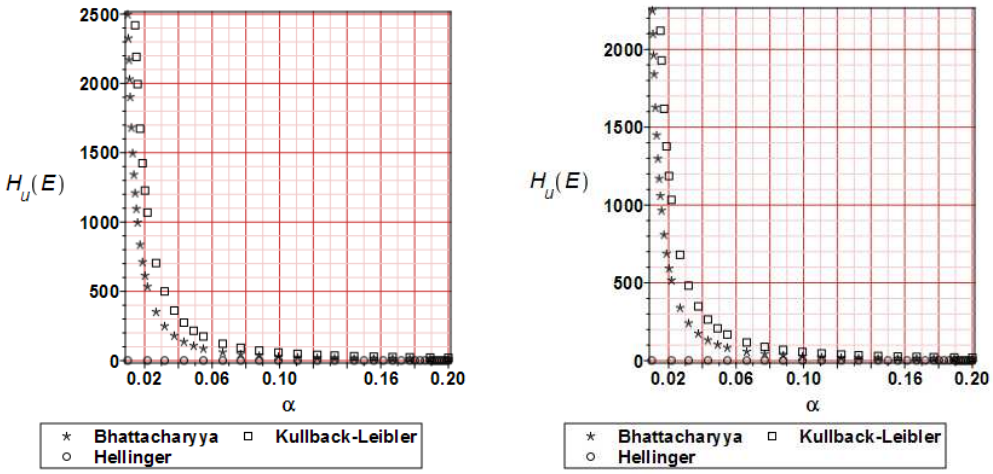

Figure 14. Relative entropy comparison for the displacements $H_u(E)$ at 20 and 80 % of the analysis progress.

Figure 15 presents the reliability index distribution for the displacements calculated based on relative entropy values; the nature of the curves is similar to Figure 14 but values are proportionally smaller. Compared with Figure 13 (left) it can be observed that the reliability index takes values 4-5 times bigger than the original relative entropy. All the curves behave in the way typical for classical reliability indices – they exponentially decrease while increasing analysis progress. A remarkable difference to the left graph of Figure 13 is that now reliability indices have remarkably larger values, so that the FORM approach returns less favorable values. Bhattacharyya model returns slightly smaller values than the Kullback-Leibler trend, while Hellinger model keeps almost constant and close to the interval [0,1].

Preprints (www.preprints.org) | NOT PEER-REVIEWED | Posted: 29 November 2023 doi:10.20944/preprints202311.1880.v1

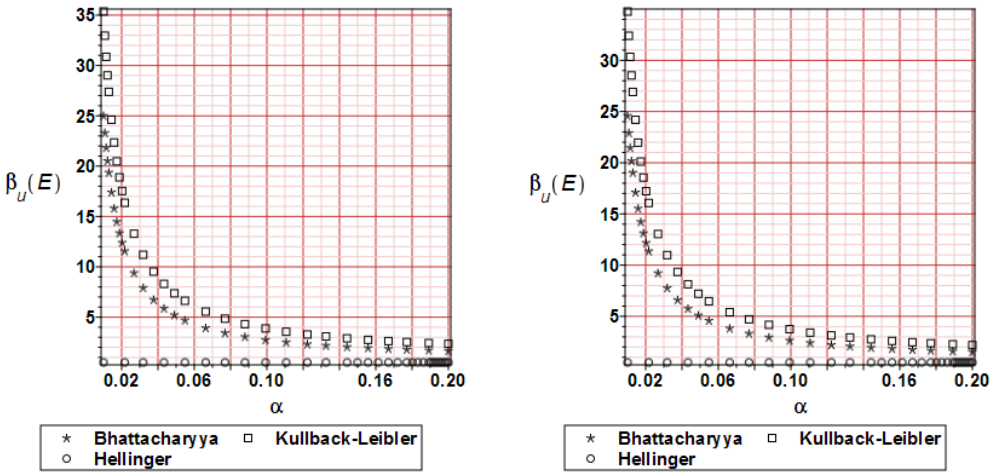

Figure 15. Reliability index $\beta_u(E)$ comparison for the displacements at 20 and 80 % of the analysis progress.

The distribution of the relative entropy for the reduced stress $H_\sigma(E)$ after 20 and 80 % of the analysis progress is presented in Figure 16. The most popular methods have been compared. As was observed for displacements Bhattacharyya and Kullback-Leibler methods bring similar character to the graphs; larger input CoV causes remarkable reduction of the entropy values. Hellinger's method leads to values close to zero throughout the entire analysis. Figure 17 shows the reliability index distribution for the reduced stress; it is based on the relative entropy course. All the curves are similar to relative entropy distribution with this note that the reliability index takes 10-15 times smaller values. Quite interestingly, their numerical values are close to numerical values obtained in the right graph of Figure 13, where the FORM reliability indices for the ULS have been presented. One may even notice that all of these trends return less favorable reliability estimation than the FORM analysis. It is seen that a difference in Kullback-Leibler model to the FORM curve is the smallest one, whereas Hellinger relative entropy returns once more less useful results because its reliability based index is less than 1. As one could expect, which agrees with engineering intuition, the reliability index based on the relative entropy remarkably decrease together with deformation process. It is obvious that probability of failure must increase while approaching to the end of numerical simulation and it is numerically proven here.

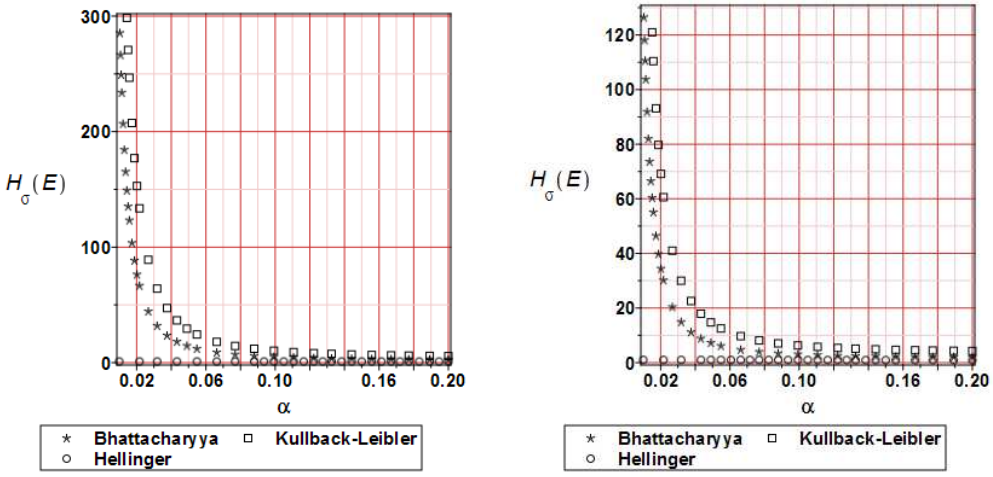

Figure 16. Relative entropy comparison for the reduced stress $H_\sigma(E)$ at 20 and 80 % of the analysis progress.

Preprints (www.preprints.org) | NOT PEER-REVIEWED | Posted: 29 November 2023 doi:10.20944/preprints202311.1880.v1

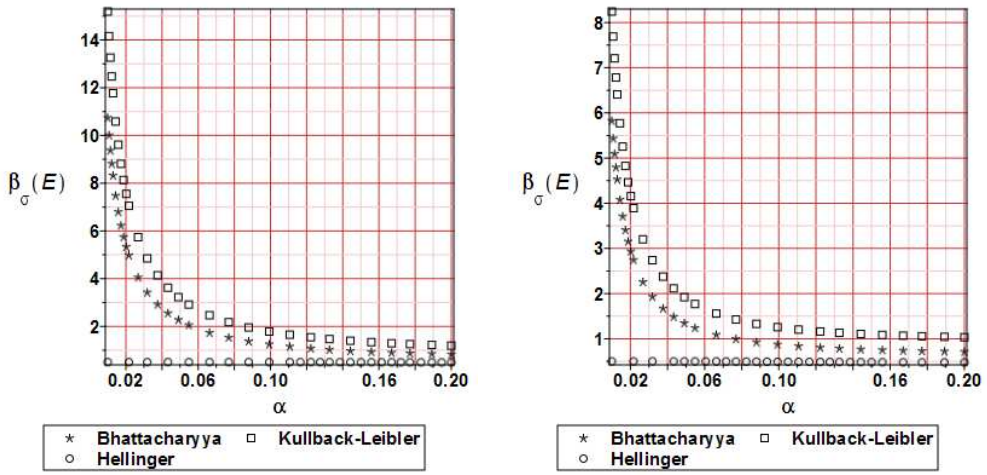

Figure 17. Reliability index $\beta_\sigma(E)$ comparison for the reduced stress at 20 and 80% of the analysis progress.

4. Concluding remarks

First, it has been demonstrated that the Stochastic Finite Element Method may be efficiently used in determination of up to the fourth order probabilistic characteristics of the structural response in computer simulation of nonlinear deformations governed by the Ramberg-Osgood material model. It can be also successively used in the reliability assessment while commonly applied with the First Order Reliability Method (FORM) or some alternative relative entropy based approach. Secondly, the first four probabilistic moments of both extreme displacements and reduced stresses have been computed using three different methodologies, namely the generalized iterative stochastic perturbation technique, Monte-Carlo simulation, and semi-analytical method. Perfect agreement of all three methods for the first two probabilistic moments confirm the usefulness of this approach, guarantees high quality of the results and enables for alternative usage of all these techniques while nonlinear problems with uncertainty are modelled. Common implementation of the FEM system ABAQUS and computer algebra software MAPLE is recommended for such a hybrid computer analysis. The following conclusions can be formulated based on the presented example and numerical results presented above:

- distribution of the reliability index β based on relative entropy and relative entropy H has similar characters but values are 10-20 times smaller for the reliability index,
- the reliability index based on relative entropy according to the Bhattacharyya and Kullback-Leiber method for the reduced stress bring numerical values quite close to the reliability index based on the FORM method,
- Jeffreys and Hellinger approximation cannot be used directly for the safety assessment,
- further work based on different steel structures should be conducted to calibrate the reliability index while using the relative entropy based methodology,
- it would be interesting and also challenging to apply this probabilistic apparatus in numerical simulation of the reliability indices for thermo-elasto-plasticity of structural steels, specifically in the context of dynamical loadings applied to the structure under consideration.

Author Contributions: M.K.; conceived and designed the experiments, M.S.; performed the experiments and analysed the data, M.K and M.S.; contributed the materials and analysis tools, M.K. and M.S.; both wrote the entire paper.

Funding: Not applicable.

Institutional Review Board Statement: Not applicable.

Informed Consent Statement: Not applicable.

Data Availability Statement: Not applicable.

Acknowledgments This paper has been written in the framework of the research grant OPUS No. 2021/41/B/ST8/02432 entitled "Probabilistic entropy in engineering computations" and sponsored by The National Science Center in Poland and the University internal grant No. 0411/SBAD/0008.

Conflicts of Interest: The authors declare no conflict of interest.

References

1. Melchers, R.E. *Structural Reliability Analysis and Prediction;* Wiley: Chichester, UK, 2002.
2. Ramberg, W.; Osgood, W. R. Description of stress–strain curves by three parameters. *Technical Note No. 902, National Advisory Committee For Aeronautics, Washington DC,* **1943**.
3. Wei, D. ; Elgindi, M.B.M. Finite element analysis of the Ramberg-Osgood bar. *Am. J. Comp. Math*. **2013**, 3, 211-216.
4. Gadamchetty, G. ; Pandey, A.; Gawture, M. On Practical implementation of the Ramberg-Osgood Model for FE Simulation. *SAE Int. J. Mat. Manuf.* **2016**, *9*, 200–205.
5. Anatolyevich, B.P.; Yakovlevna, G.N. Generalization of the Ramberg–Osgood Model for Elastoplastic Materials. *J. Mat. Engrg. Perform.* **2019,** *28*, 7342–7346.
6. Elruby, A.Y.; Nakhla, S. Extending the Ramberg–Osgood Relationship to Account for Metal Porosity. *Metall Mater. Trans. A* **2019**, *50*, 3121–3131.
7. Skelton, R.P.; Maier, H.J.; Christ, H.-J. The Bauschinger effect, Masing model and the Ramberg–Osgood relation for cyclic deformation in metals. *Materi. Sci. Eng.* **1997**, *238*, 377-390.
8. Li, J.; Zhang, Z.; Li, C. An improved method for estimation of Ramberg–Osgood curves of steels from monotonic tensile properties. *Fat. & Frac. Eng. Mat. Struct*. **2016**, *39*, 412-426.
9. Niesłony, A.; el Dsoki, Ch.; Kaufmann, H.; Krug, P. New method for evaluation of the Manson–Coffin–Basquin and Ramberg–Osgood equations with respect to compatibility. *Int. J. Fat*. **2008**, *30*, 1967-1977.
10. Basan, R.; Fralunović, M.; Prebil, I.; Kunc, R. Study on Ramberg-Osgood and Chaboche models for 42CrMo4 steel and some approximations. *J. Constr. Steel Res*. **2017**, *136*, 65-74.
11. Kaldjiian, M.J. Moment-Curvature of Beams as Ramberg-Osgood Functions. *J. Struct. Div*. **1967**, *93*.
12. Mostaghel, N.; Byrd, R.A. Inversion of Ramberg–Osgood equation and description of hysteresis loops. *Int. J. N-Lin. Mech*. **2002**, *37*, 1319-1335.
13. Papadimitriou, A.G.; Buckovalas, G.D. Plasticity model for sand under small and large cyclic strains: a multiaxial formulation. *Soil Dyn. Earthq. Engrg*. **2002**, *22*, 191-204.
14. Wang, X.; Shi, J.; Validation of Johnson-Cook plasticity and damage model using impact experiment. *Int. J. Impact Engrg*. **2013**, *60*, 67-75.
15. Strąkowski, M.; Kamiński, M. Stochastic Finite Element Method elasto-plastic analysis of the necking bar with material microdefects. *ASCE-ASME J. Risk Uncert. Eng. Sys. Part B Mech. Eng*. **2019**, *5*, 030908.
16. Kossakowski, P. The numerical modeling of failure of 235JR steel using Gurson-Tvergaard-Needleman material model. *Roads & Bridges* **2012**, *11*, 295–310.
17. Qu, P.; Sun, Y.; Sumelka, W. Review on Stress-Fractional Plasticity Models. *Materials* **2022**, *15*, 7802.
18. Buryachenko, V. 1999, Elastic-plastic behavior of elastically homogeneous materials with a random field of inclusions. *Int. J. Plast.* **1999**, *15*, 687–720.
19. Kamiński, M. Probabilistic characterization of porous plasticity in solids. *Mech. Res. Comm.* **1999**, *26*, 99–106.
20. Kamiński, M. *The Stochastic Perturbation Method for Computational Mechanic;* Wiley: Chichester, UK, 2013.
21. Hamada, M.S.; Wilson, A.G.; Reese, C.S.; Martz, H.F. *Bayesian Reliability*. Springer Series in Statistics, Berlin-Heidelberg, **2008**.
22. Cardoso, J.B.; de Almeida, J.R.; Dias, J.M.; Coelho, P.G.; Structural reliability analysis using Monte Carlo simulation and neural networks. *Adv. Engrg. Software* **2008**, *39*, 505-513.
23. Ghanem, R.; Spanos, P.D. *Stochastic Finite Elements: A Spectral Approach*; Springer Verlag: Berlin-Heidelberg, Germany,**1991**.
24. Kleiber, M.; Hien, T.D. *The Stochastic Finite Element Method*; Wiley: Chichester, UK, 1992.
25. Shannon, C.E. A mathematical theory of communication. *Bell Sys. Tech. J.* **1948**, *27*, 379-423; doi:10.1002/j.1538-7305.1948.tb01338.x.
26. Renyi, A. On measures of information and entropy. *Proc. Fourth Berkeley Symp. Math., Stat. Prob.* **1960**, 547-561.
27. Tsallis, C. Possible generalization of Boltzmann-Gibbs statistics. *J. Stat. Phys.* **1988**, *52*, 479-487.
28. Zhao, Y-G.; Ono, T. Moment methods for structural reliability. *Struct. Safety* **2001**, *23*, 47-75.
29. Lopez, R.H.; Beck, A.T. Reliability-Based Design Optimization Strategies Based on FORM: A Review. *J. Braz. Soc. Mech. Sc. Eng.* **2012**, *34*, 506-514.
30. Cai, G.Q.; Elishakoff, I., Refined second-order reliability analysis. *Struct. Safety* **1994**; *14*, 267-276.
31. Tichy, M. First-order third-moment reliability method. *Struct. Safety* **1994**, *16*, 189-200.

32. Peng, X. ; Geng, L. ; Liyan, W. *et al.* A stochastic finite element method for fatigue reliability analysis of gear teeth subjected to bending. *Comput. Mech.* **1988**, *21*, 253–261; https://doi.org/10.1007/s004660050300.
33. Donald, M.J. On the relative entropy. *Comm. Math. Phys*. **1986**, *105*, 13-34.
34. *Bhattacharyya, A. On a measure of divergence between two statistical populations defined by their probability distributions. Bull. Calcutta Math. Soc.* ***1943****, 35, 99–109.*
35. Hellinger, E. Neue Begründung der Theorie quadratischer Formen von unendlichvielen Veränderlichen. *J. fűr die Reine & Angew. Math. (Crelles Journal)*, **1909**, *136*, 210–271.
36. Jeffreys, H. An invariant form for the prior probability in estimation problems. *Proc. Roy. Soc. London. Ser. A, Math. & Phys. Sci.* **1946**, *186*, 453-461.
37. Nielsen, F. Fast approximations of the Jeffreys divergence between univariate Gaussian mixtures via mixture conversions to exponential-polynomial distributions. *Entropy,* **2021**, *23*, 1417.
38. Kullback, S.; Leibler, R.A. On information and sufficiency. *Ann. Math. Stat.* **1951**, *22*, 79–86.
39. Teixeira, R.; O'Connor, A.; Nogal, M. Probabilistic Sensitivity Analysis of OWT using a transformed Kullback-Leibler discrimination. *Struct. Safety* **2019**, *81*, 101860.
40. Ghasemi, S.H.; Nowak, A.S. Reliability index for non-normal distributions of limit state functions. *Struct. Eng. Mech*. **2017**, *62,* 365-372.
41. Kleiber, M.; Woźniak, Cz. *Nonlinear Mechanics of Structures*; Kluwer Academic Publishers: Dordrecht, Netherlands, 1991.
42. Oden, J.T. *Finite Elements of Nonlinear Continua*; McGraw-Hill: New York, NY, USA, 1972.
43. Zienkiewicz, O.C.; Taylor, R.C. *The Finite Element Method*, 4th ed; McGraw Hill: New York, NY, USA, 1989.
44. Bjorck, A. *Numerical Methods for Least Squares Problems*; SIAM: Philadelphia, PA, USA, 1996.
45. Aravas, N. On the numerical integration of a class of pressure-dependent plasticity models. *Int. J. Num. Meth. Eng.* **1987**, *24*, 1395–1416.